Automatic seagrass pattern identification on Sonar images

Maryam Rahnemoonfar[1], Abdullah Rahman[2]

1: School of Engineering and Computing Sciences, Texas A&M University-Corpus Christi

2: Coastal Studies Lab, University of Texas Rio Grande Valley

ABSTRACT

Natural and human-induced disturbances are resulting in degradation and loss of seagrass. Freshwater flooding, severe meteorological events and invasive species are among the major natural disturbances. Human-induced disturbances are mainly due to boat propeller scars in the shallow seagrass meadows and anchor scars in the deeper areas. Therefore, there is a vital need to map seagrass ecosystems in order to determine worldwide abundance and distribution. Currently there is no established method for mapping the pothole or scars in seagrass. One of the most precise sensors to map the seagrass disturbance is side scan sonar. Here we propose an automatic method which detects seagrass potholes in sonar images. Side scan sonar images are notorious for having speckle noise and uneven illumination across the image. Moreover, disturbance presents complex patterns where most segmentation techniques will fail. In this paper, by applying mathematical morphology technique and calculating the local standard deviation of the image, the images were enhanced and the pothole patterns were identified. The proposed method was applied on sonar images taken from Laguna Madre in Texas. Experimental results show the effectiveness of the proposed method.

Keywords- Seagrass, Sonar, Pattern recognition, Mathematical morphology

1. INTRODUCTION

The widespread loss of seagrass beds is largely caused by the rapid expansion of human populations around coastal waterways [1]. There is a vital need to map seagrass ecosystems in order to determine worldwide abundance and distribution. A variety of remote sensing approaches have been used for mapping and observing seagrass since the 1990s [2-9] . Detection of seagrass with optical remote sensing (both satellite imagery and aerial photography) is complex due to the fact that light is attenuated as it passes through the water column and reflects back from the benthos. Therefore, optical remote sensing of seagrass is only possible if the water is shallow and relatively clear. In reality, coastal waters are commonly turbid, and seagrasses can grow under 10 meters of water or even deeper. Previous researches on sonar images have mainly focused on detecting concrete objects on sandy sea floor [10] [11] [12] [13] [14] . Although the side scan sonar has been used for benthic mapping there is no existing method that automatically detects the extent of seagrass beds or automatically identifies and maps its disturbance.

We collected sonar images in Laguna Madre which contains 75% of the seagrass of Texas's coastline. Underwater acoustics mapping produces a high definition, two-dimensional sonar image of seagrass ecosystems. To identify disturbances in seagrass structure, we propose a novel technique based on mathematical morphology and local standard deviation for recognition of potholes on seagrass structure depicted on sonar images. To the best of our knowledge this research is the first of its kind on seagrass disturbance identification using sonar. Sonar images usually suffer from non-uniform illumination which makes a real challenge in the segmentation of natural and man-made disturbance in sea-grass. Moreover, disturbance presents complex patterns where most segmentation techniques would normally fail.

Automatic Target Recognition XXVI, edited by Firooz A. Sadjadi, Abhijit Mahalanobis,
Proc. of SPIE Vol. 9844, 98440C · © 2016 SPIE · CCC code: 0277-786X/16/$18 · doi: 10.1117/12.2224191

The detail of our algorithm is presented in section 2. Experimental results are presented in section 3 and conclusion is drawn in section 4.

2. PROPOSED METHOD

Our algorithm consists of two major steps; In the first step, the uneven illumination is reduced and the image is enhanced based on Top-hat transformation and Gaussian adaptive thresholding. In the next step, seagrass disturbance patterns are identified based on calculating local standard deviation and applying closing and opening morphological operators.

2.1 Image enhancement

Side scan sonar uses two parallel transducers to transfer a high frequency acoustic signal in the water. Side-scan sonar images often show striking variations in brightness due to the fact that objects closer to the transducer will create higher reflections. Figure 1 shows a sonar image. As it can be seen in Figure 1 the brightness values varies across the image. In the middle of the image, where the boat is moving there is higher intensity of reflection and the image is bright while in the side of the image, the reflection is of lower intensity and the image looks darker.

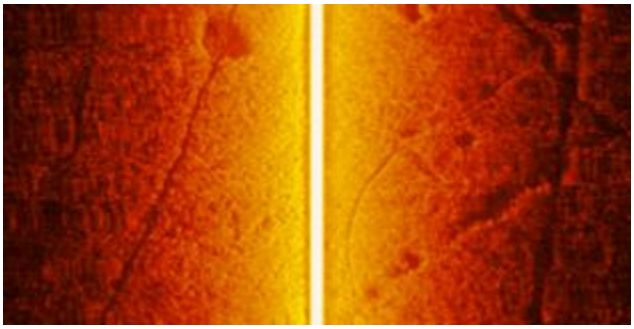

Figure 1: Sidesacn sonar image with uneven illumination across the image

To remove the uneven illumination defects in the image we used several enhancement filters including Top-hat mathematical morphology filter. Mathematical morphology offers a unified and powerful approach to numerous image processing problem. The language of mathematical morphology is set theory. In binary images, the set elements are members of the 2-D integer space – Z^2, where each element *(x,y)* is a coordinate of a black (or white) pixel in the image. To remove the non-uniform illumination from sonar images, we used mathematical morphology top-hat transformation which is defined as the function minus its opening:

$$T_{hat}(f) = f - (f \circ b) \tag{1}$$

Where *f* is the original image, *b* is the structure element and $\circ$ is opening morphological operator. Opening of *A* by *B* is the erosion of *A* by *B* followed by dilation of the result by *B*. Structure elements are small sets or sub images used to probe an image under study. Here, the structure element is circle with radius of 50 pixels. Figure 2 shows the result of applying top-hat transform on the original image. Figure 2a shows the original image. Figure 2b shows the opening morphological image and Figure 2c shows the result of top-hat transform on the original image. As it can be seen in figure 2c, the illumination is distributed more evenly.

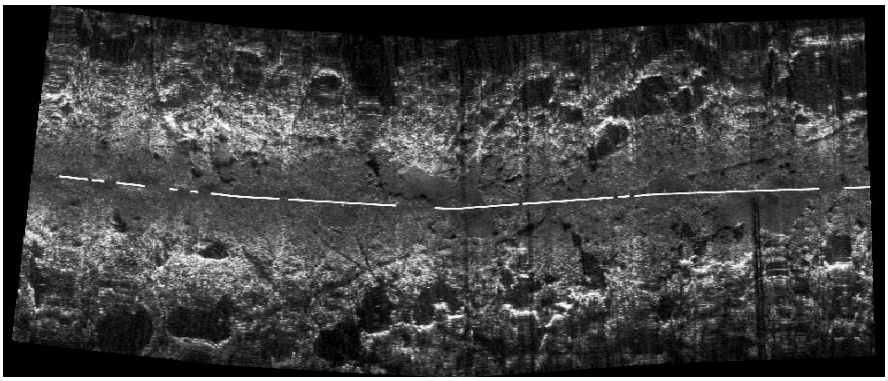

(a)

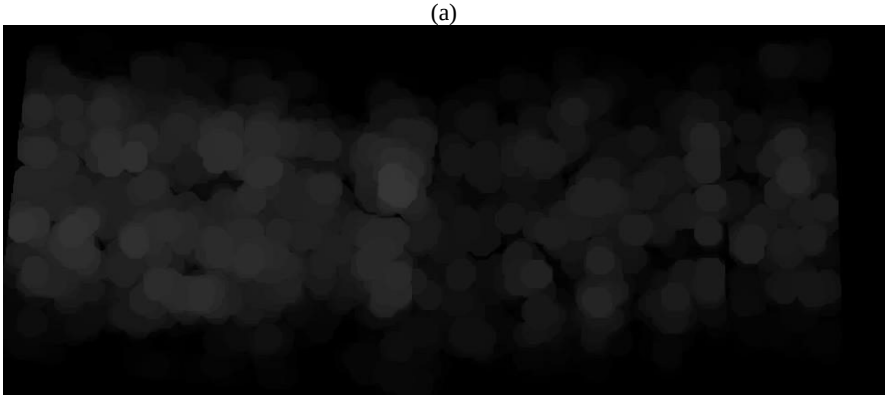

(b)

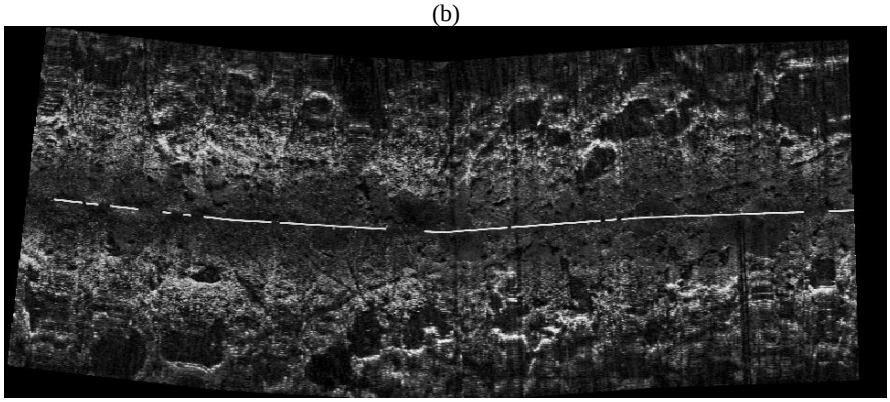

(c)

Figure 2: removing uneven illumination using top-hat transform. a)Original image, b) opening morphological filter c) top-hat transform

To further enhance the image and reduce the non-uniformities in reflectance, we applied Gaussian adaptive thresholding technique. In this method, a variable threshold was calculated at every point, (x,y) based on the properties computed in a neighborhood of (x,y). In Gaussian adaptive thresholding, the threshold value is a weighted sum of the small neighborhood around pixel. The neighborhood windows are chosen small enough so that the illumination of each is approximately uniform. A threshold is calculated for each pixel based on the convolution of the image with Gaussian function as following:

$$T(x,y) = \sum_{k=-a}^{a} \sum_{l=-b}^{b} G(s,t) f(x-k, y-l) \tag{2}$$

where G is the Gaussian function of two variables and has the basic form of

$$G(x,y)=\frac{1}{2\pi\sigma^2}e^{-\frac{x^2+y^2}{2\sigma^2}} \tag{3}$$

where σ is the standard deviation.

Figure 3 shows the result after applying adaptive thresholding on the image in figure 2c.

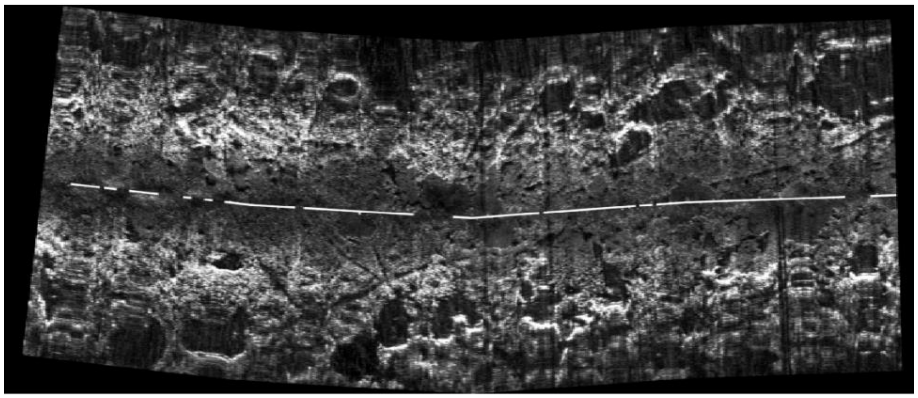

Figure 3: The result of applying Gaussian adaptive thersholding.

2.2 Seagrass pattern identification

After enhancing the image and removing the effect of ununiformed illumination, the process of extracting pothole in sonar images will be conducted.

To extract pothole in seagass, the local standard deviation of the image was calculated according to the following formula:

$$\sigma^2(i,j)=\frac{1}{(2n+1)^2}\sum_{k=i-n}^{i+n}\sum_{l=j-n}^{j+n}[g(k,l)-m\ (i,j)]^2 \tag{4}$$

Where g is the gray value of pixel, and local window is defined over a $(2n+1)\times(2n+1)$ area and m is the average of pixels' grey value in the local window. Local standard deviation shows the high frequency component at each pixel and highlights the pothole boundaries. After binarizing the image, closing morphological filter was applied on the binarized image. Closing of *A* by *B* is the dilation of *A* by *B* followed by erosion of the result by *B*:

$$A\bullet B=(A\oplus B)\ominus B \tag{5}$$

Closing smooths sections of contours, eliminate small holes, and fills gaps in the contour. Here we used circle with diameter of 11 pixels as our structural elements. At the final stage, the boundary of objects in the image is calculated using the following formula:

$$\beta(A)=A-(A\ominus B) \tag{6}$$

Where A is the original image, and $\ominus$ is the erosion mathematical morphology operator.

3. EXPERIMENTAL RESULTS

The data was collected in Laguna Madre which contains 75% of the seagrass of Texas's coastline. To collect data, we built a prototype side scan sonar.

We used two Lowrance Structure Scan HD LSS-2 transduces as our side scan transducers. These transducers can produce 455 KHz and 800 KHz frequencies. Our bathymetric sounder is a Dual Beam 200 KHz transducer. Boat's position is measured with a GPS receiver, and the water's depth is determined using a bathymetric sounder. Navigation information is recorded continuously along with the reflected acoustic signals. Combining each line of reflected signal with its position, time and depth, and mosaicking all lines in the chronological sequence produces an image of the seafloor (Figure 1).

Figure 4 shows the result of the proposed method. Figure 4a shows the enhanced image which would be the input to the pattern recognition step. Figure 4b is the results of local standard deviation on the enhanced image of Figure 4a. As it can be seen in figure 4b, the high frequency features are highlighted in the image. Figure 4c shows the result after binarization and closing filter. Figure 4d delineate the boundary of seagrass after applying the boundary detection filter. Figure 4e, highlights the seagrass. The magnified sections of Figure 4d is depicted in Figures 4f and 4g. As it can be seen in Figures 4f and 4g, the proposed method accurately and automatically delineated the boundary of seagrass and pothole in seagrass.

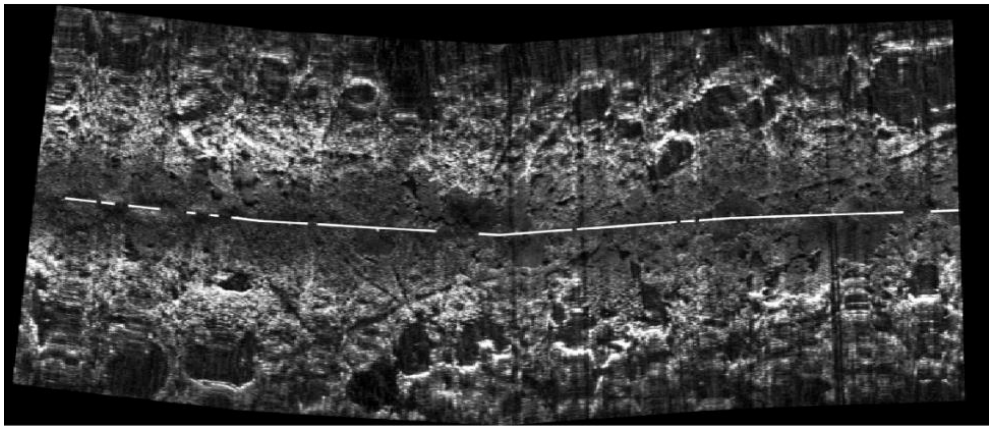

(a)

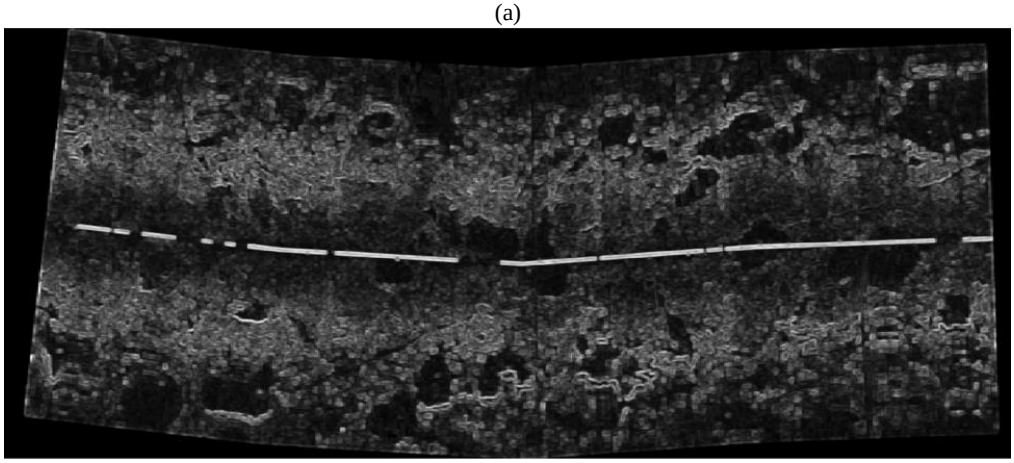

(b)

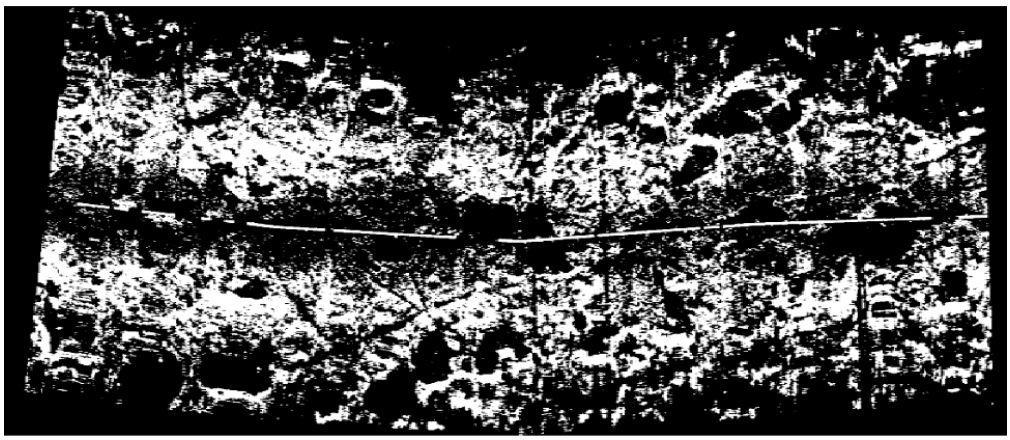

(c)

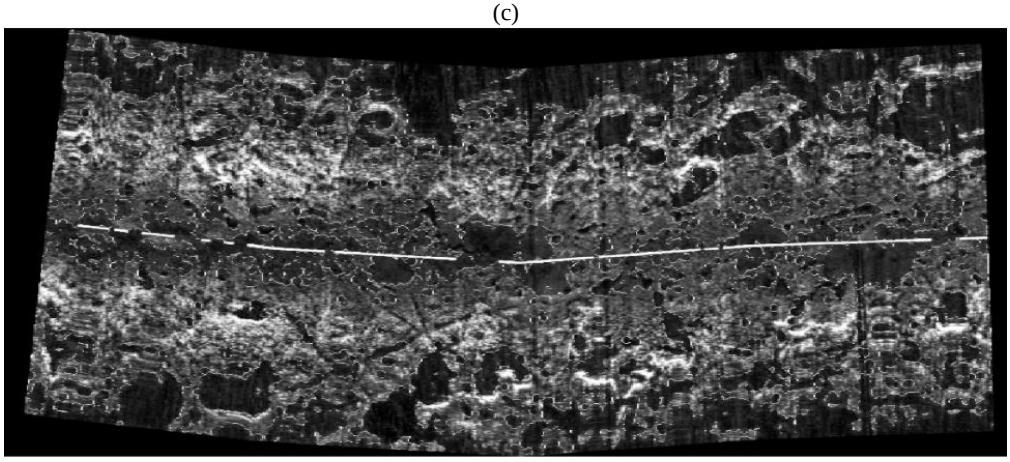

(d)

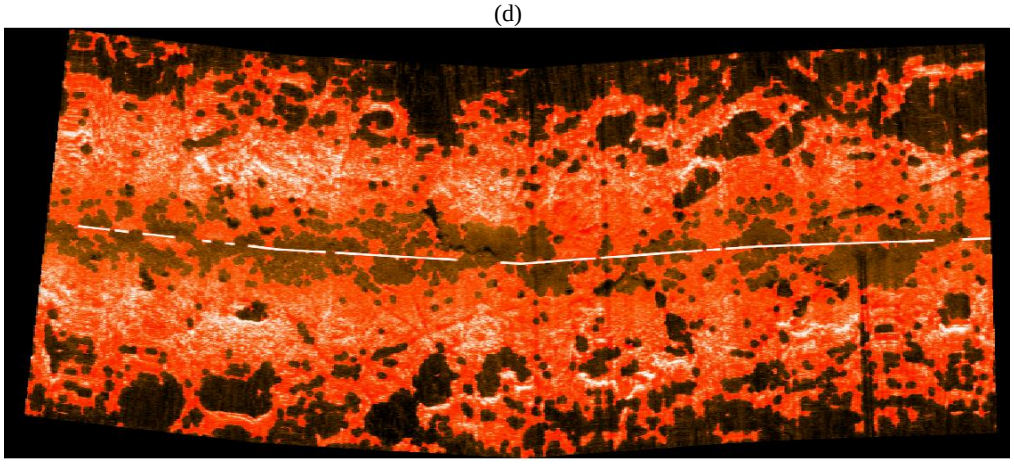

(e)

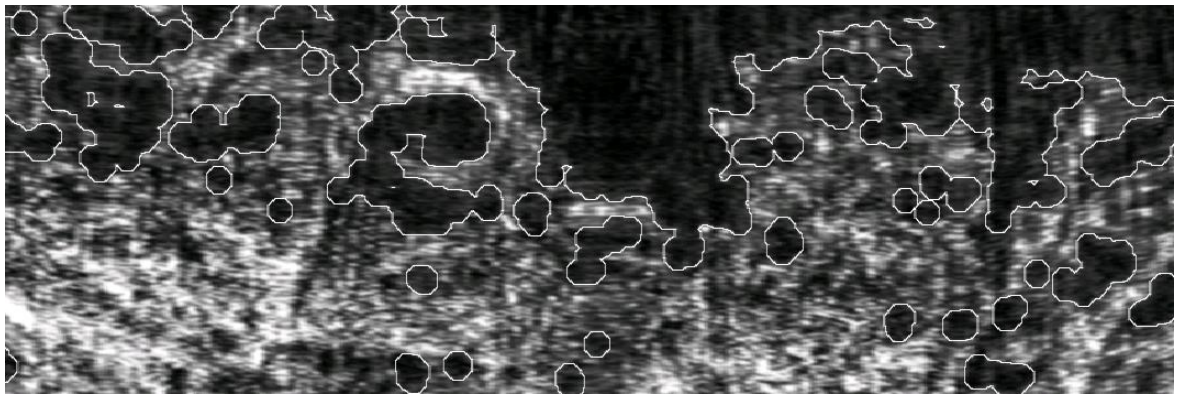

(f)

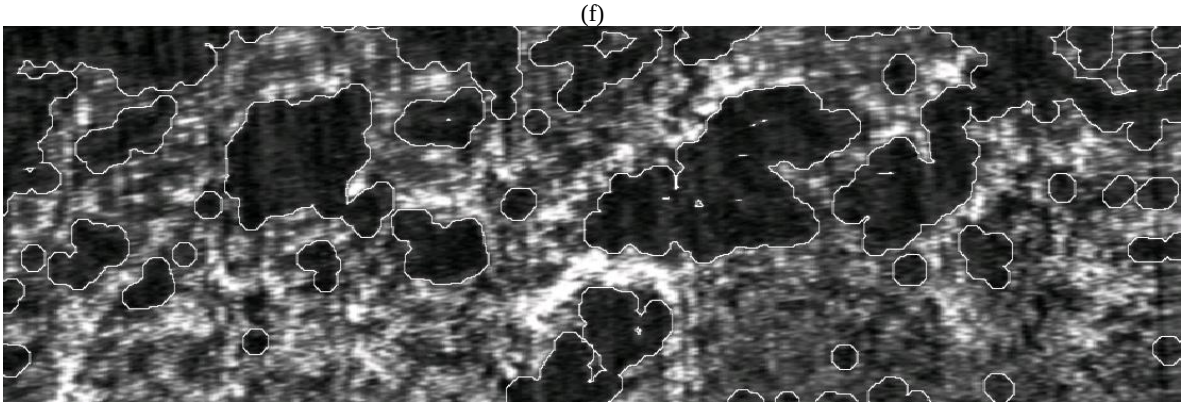

(g)

Figure 4: The result of the proposed methodology on dataset 1, a) enhanced image, b) local standard deviation, c) the image after binarization and closing filter, d) boundary of pothole areas, e) highlighted seagrass, f-g) magnified sections of image d.

Figure 5 demonstrates the result for a vertical sonar scanning. Figure 5a shows the original image. Figure 5b shows the enhanced image after top-hat transform. There are still some non-uniformities in this image. After further enhancement using adaptive Gaussian threshold, we got the image in figure 5c. To extract the pothole boundaries, local standard deviation is applied in figure 5d. Figure 5e shows the image after binarization and closing filter. Figure 5f highlights the seargrass and finally Figure 5g shows the magnified sections of image.

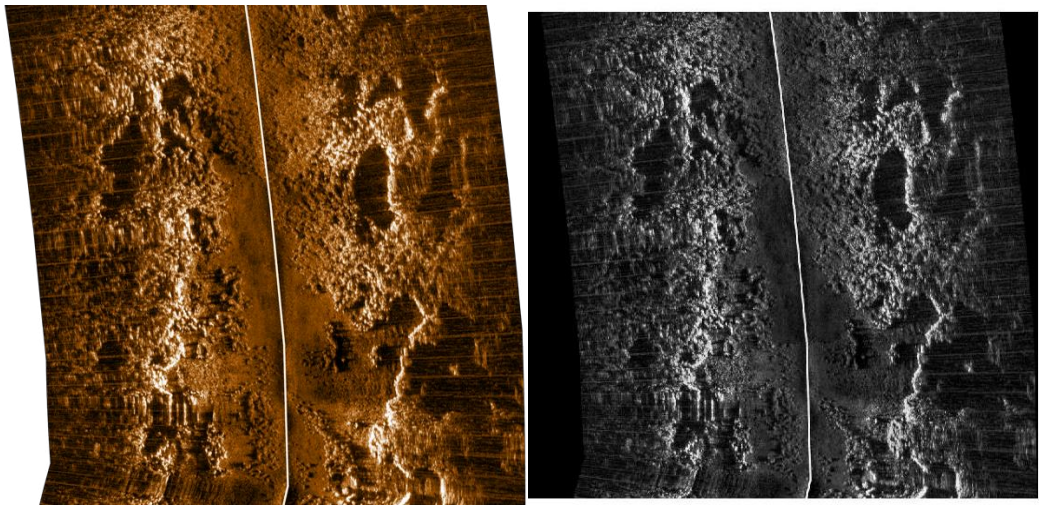

(a) (b)

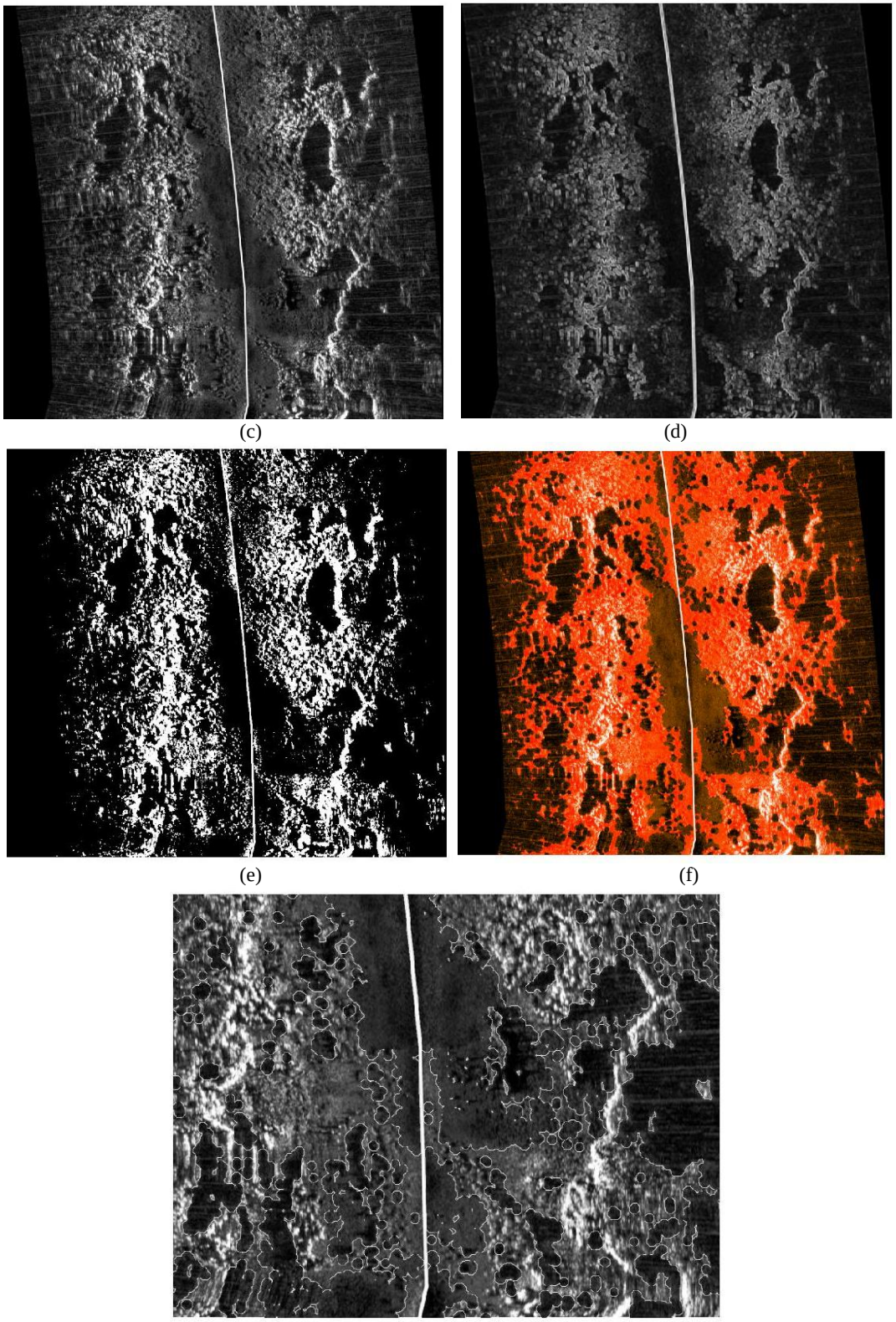

Figure 5: The result of the proposed methodology on dataset 2, a) original image, b) enhanced image after top-hat transform, c) enhanced image after adaptive filtering d) local standard deviation, e) the image after binarization and closing filter, (f) highlighted seagrass, g) magnified sections of image (f)

4. CONCLUSION

In this paper, we proposed an automated method to detect seagrass potholes using sonar imagery. Presence of uneven illumination and noise in sonar images puts forth a big obstacle in recognition of any pattern in the images. Our method combines adaptive thresholding and top-hat mathematical transform to remove image noises and irregularities. Then, we designed a wholly automatic technique to detect the boundary of potholes using local standard deviation and mathematical morphology filters. The proposed method shows promising results as we applied it to sonar images taken from Laguna Madre in Texas. Our method has successfully detected pothole boundaries and seagrass disturbance patterns in our sonar images.

5. REFERENCES

[1] H. K. Lotze, H. S. Lenihan, B. J. Bourque, R. H. Bradbury, R. G. Cooke, M. C. Kay, *et al.*, "Depletion, degradation, and recovery potential of estuaries and coastal seas," *Science*, vol. 312, pp. 1806-1809, 2006.

[2] M. Hossain, J. Bujang, M. Zakaria, and M. Hashim, "Assessment of Landsat 7 Scan Line Corrector-off data gap-filling methods for seagrass distribution mapping," *International Journal of Remote Sensing*, vol. 36, pp. 1188-1215, 2015.

[3] A. G. Dekker, V. E. Brando, and J. M. Anstee, "Retrospective seagrass change detection in a shallow coastal tidal Australian lake," *Remote Sensing of Environment*, vol. 97, pp. 415-433, 9/15/ 2005.

[4] H. M. Dierssen, A. Chlus, and B. Russell, "Hyperspectral discrimination of floating mats of seagrass wrack and the macroalgae Sargassum in coastal waters of Greater Florida Bay using airborne remote sensing," *Remote Sensing of Environment*, vol. 167, pp. 247-258, 9/15/ 2015.

[5] J. Hedley, B. Russell, K. Randolph, and H. Dierssen, "A physics-based method for the remote sensing of seagrasses," *Remote Sensing of Environment*, vol. 174, pp. 134-147, 3/1/ 2016.

[6] V. Pasqualini, C. Pergent-Martini, G. Pergent, M. Agreil, G. Skoufas, L. Sourbes, *et al.*, "Use of SPOT 5 for mapping seagrasses: An application to Posidonia oceanica," *Remote Sensing of Environment*, vol. 94, pp. 39-45, 1/15/ 2005.

[7] S. Phinn, C. Roelfsema, A. Dekker, V. Brando, and J. Anstee, "Mapping seagrass species, cover and biomass in shallow waters: An assessment of satellite multi-spectral and airborne hyper-spectral imaging systems in Moreton Bay (Australia)," *Remote Sensing of Environment*, vol. 112, pp. 3413-3425, 8/15/ 2008.

[8] C. M. Roelfsema, M. Lyons, E. M. Kovacs, P. Maxwell, M. I. Saunders, J. Samper-Villarreal, *et al.*, "Multi-temporal mapping of seagrass cover, species and biomass: A semi-automated object based image analysis approach," *Remote Sensing of Environment*, vol. 150, pp. 172-187, 7// 2014.

[9] C. C. Wabnitz, S. Andréfouët, D. Torres-Pulliza, F. E. Müller-Karger, and P. A. Kramer, "Regional-scale seagrass habitat mapping in the Wider Caribbean region using Landsat sensors: Applications to conservation and ecology," *Remote Sensing of Environment*, vol. 112, pp. 3455-3467, 8/15/ 2008.

[10] M. Mignotte, Collet, C., Perez, P., Bouthemy, P.,, "Three-class Markovian segmentation of high-resolution sonar images.," *Computer Vision and Image Understanding*, vol. 76 (3). pp. 191-204, 1999.

[11] M. Mignotte, Collet, C., Perez, P., Bouthemy, P.,, "Sonar Image Segmentation Using an Unsupervised hierarchical MRF Model," *IEEE Transactions on Image Processing*, vol. 9 pp. 1216-1231., 2000.

[12] M. Lianantonakis, Petillot, Y.R.,, "Sidescan sonar segmentation using active contours and level set methods," presented at the Oceans 2005, Europe, 2005.

[13] W. Tian, "Automatic Target Detection and Analyses in Side-scan Sonar Imagery," presented at the WRI Global Congress on Intelligent Systems, 2009. GCIS '09., 2009.

[14] X.-F. Ye, Z.-H. Zhang, P. X. Liu, and H.-L. Guan, "Sonar image segmentation based on GMRF and level-set models," *Ocean Engineering,* vol. 37, pp. 891-901, 2010.